

A common cause failure model for components under age-related degradation



Taotao Zhou^{a,*}, Enrique López Droguett^{a,b}, Mohammad Modarres^a

^a Center for Risk and Reliability, University of Maryland, College Park, MD, United States

^b Department of Mechanical Engineering, University of Chile, Santiago, Chile

ARTICLE INFO

Keywords:

Common cause failures
Condition monitoring
Age
Degradation
Imperfect maintenance

ABSTRACT

This paper discusses component age-related degradation and failure initiated from a shared cause and coupling factor (or mechanism) and the likelihood of the resulting common cause failure (CCF). For these components a CCF model that includes the impacts of any maintenance-related renewal is proposed. Limitations and gaps in the state-of-the-art parametric CCF models for properly handling impacts of shared causes leading to accelerated degradation and aging have been discussed. The proposed approach characterizes the likelihood of CCF based on the conventional parametric CCF model, but unlike the parametric CCF models, time-dependent CCF parameters are estimated from the degradation states including any component rejuvenation achieved through preventive maintenance. Accelerated degradation tests of three identical centrifugal pumps under shared but harsh operating conditions generated several types of sensor monitoring data until failure. Correlation between the sensor monitoring data and observed aging and pump failure times were used to infer the degradation states of the pumps tested. The results concluded that undetected shared causes that could accelerate degradation and aging, for example due to poor maintenance, could significantly affect the CCF parametric model and CCF probability. This could potentially underestimate risk estimates as the undetected components degradation accumulates. The proposed parametric CCF model would be able to determine component-specific dynamic CCF probability, for condition monitored components using sensor information relatable to degradation and aging.

1. Introduction

Dependent failures that result from *shared causes* encompass the possible mechanisms that directly compromise component performances and ultimately accelerate or trigger degradation or failure of multiple components are referred to as common cause failure (CCF) events [1]. A class of common cause dependencies referred to as the extrinsic dependency coupling that are not inherent or intended in the functional characteristics of the component, if not detected and corrected, usually lead to rapid degradation and aging in components. Extrinsic common cause dependencies originate from shared physical or environment stresses, human interventions (e.g., due to poor maintenance or positioning the component in an improper operating state). Shared causes that lead to CCF have two elements: a root cause and a coupling factor (or more appropriately in the context of this paper, a mechanistic-based coupling). The shared root cause is the fundamental source that trigger CCF and, if corrected, would terminate the possibility of failure its recurrence. The coupling factor describes the mechanism that makes multiple components susceptible to the same root

cause. A class of operation or maintenance-related root causes, for example common inadequate maintenance actions on multiple redundant components involving minor misalignment of a rotating shaft could initiate a long-term wear degradation process (i.e., the coupling mechanism shared by these components), lead to rapid degradation and ultimate CCF of components. These root causes of CCF that trigger or accelerate degradation (i.e., as will be shown later in this paper), lead to a time-dependent parametric common cause model. Under these coupled mechanism conditions, the likelihood of multiple near simultaneous failures (i.e., CCF) although low at first, it will increase over time as degradation progresses if not corrected. Similarly, internal and external exposure outside the design envelope or energetic events such as earthquake, fire, flooding could also act as triggering root causes leading to common coupling factors (i.e., accelerated aging and degradation mechanisms). In summary, this paper focuses on the subclass of multiple dependent component failures due to a shared root cause that triggers or accelerates degradation mechanisms in those components.

In the literature, the relevant CCF models [2] may be grouped into

* Corresponding author.

E-mail address: ttz@umd.edu (T. Zhou).

<https://doi.org/10.1016/j.ress.2019.106699>

Received 22 March 2018; Received in revised form 2 July 2019; Accepted 12 October 2019

Available online 14 October 2019

0951-8320/ © 2019 Elsevier Ltd. All rights reserved.

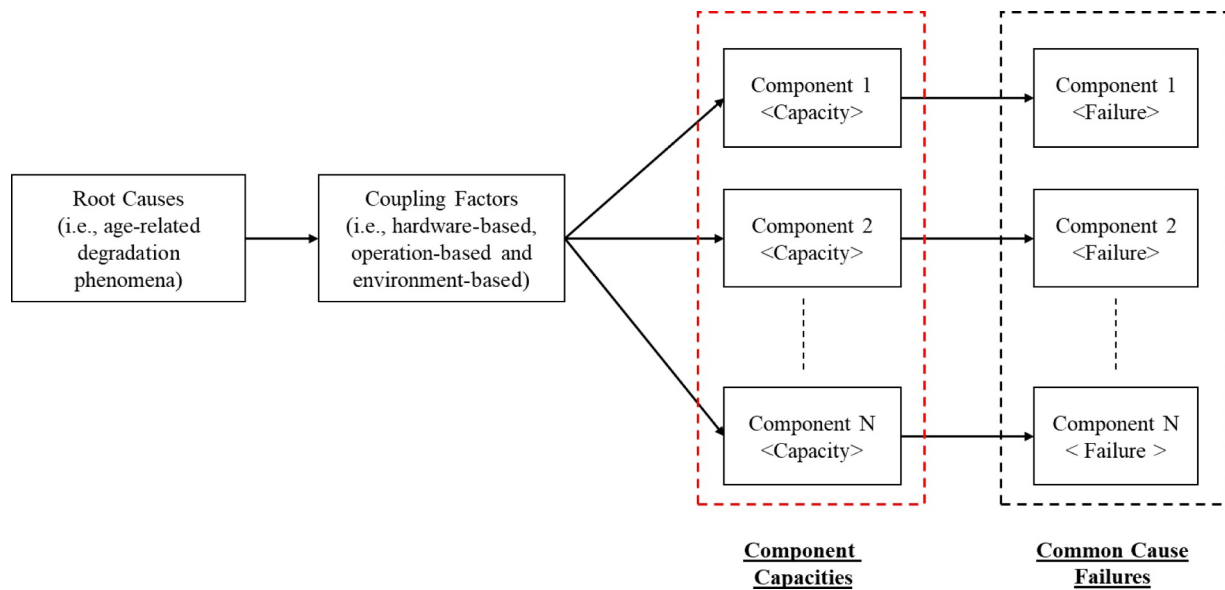


Fig. 1. CCF for components under age-related degradation.

two major categories: shock models (e.g., binomial failure rate model) and non-shock models. The non-shock models, including the β -factor model, the α -factor model and the multiple Greek letter model, have been widely adopted in probabilistic risk assessment (PRA) practices [3]. In these models, the CCF events are characterized by some static CCF parameters that need to be quantified through statistical analysis based on historical observations and engineering judgment [4,5]. However, these CCF models suffer from several major limitations summarized as follows:

- The models are built mainly from generic operational experience and are usually not specific to the operating conditions of individual components.
- The number of observed failure events, particularly in the nuclear power plants is very limited, especially for the events involving failures of more than one identical or similar component.
- It is difficult to model asymmetrical components and to account for the dependencies among the components within multiple common cause component groups.

To address these limitations, four main approaches in the present literature have been reported to enhance these CCF models:

- Improve the quality and quantity of CCF database by compiling the CCF event data in a more consistent manner. For example, the International Common-Cause Failure Data Exchange (ICDE) Project [6] was established to obtain both qualitative and quantitative insights of CCF by properly integrating many international experiences.
- Formulate a causal model for CCF, rather than the conventional parametric model to account for the relationship of specific root causes and coupling factors on the CCF events. A Bayesian network is usually adopted to establish the causal framework to probabilistically link all relevant sources. Examples include the unified partial method and its extension, referred to as the Zitrou's model [7], the Kelly-CCF method [8], the alpha-decomposition method [9], and the general dependency model [10].
- Extend the scope of the current parametric CCF to include both the identical and diverse component groups: for example, from multiple nuclear reactor units on a common site. This includes the recent works of Fleming [11], Ebisawa et al. [12], and Modarres et al. [13,14].

- Address other limitations of the current CCF models: for instance, by treating the dependencies among the components across multiple common cause component groups [15,16], improving the uncertainty treatment [17,18], and developing the extension of current CCF models [19,20].

The above approaches do not explicitly consider the aging impact of degradation mechanisms triggered or accelerated by shared root causes that would substantially contribute to CCF. Addressing this concern constitutes the primary objective of this study in which the proposed models are validated by degradation related information that are experimentally inferred through condition monitoring data of identical pumps. The components in the nuclear industry are subject to normal plant aging mechanisms where effects of CCF would be paramount [21]. Research efforts presented by US NRC [22], IAEA [23,24] and CNSC [25] discuss these concerns.

The concept introduced in this paper is different than the normal aging and degradation processes that increase the likelihood of independent failure events over time. Normal aging occurs slowly due to the expected environmental and operational conditions, that is often the result of less than perfect renewal during maintenance actions. However, some shared root causes could accelerate these aging mechanisms or trigger new underlying degradation and aging mechanisms that contribute to degradation-induced CCF.

It is important to investigate the dynamic characteristics of CCF for components undergoing age-related degradation (e.g., wear, corrosion, fatigue, erosion). As displayed in Fig. 1, a class of CCF events are caused by age-related degradation processes [26] that result in cumulative degradation in multiple components, impairing their capacities (i.e., component tolerance to withstand cumulative degradation) to perform their designed functions. Typically, the common cause dependencies are characterized [2] by three related root causes—pre-operational, operational-maintenance and operational-environment-related—and three coupling factors—hardware-based, operation-based and environment-based. While the root causes of most CCF events are attributed to age-related degradation processes [26], other root causes involving extreme loads and shock impacts (e.g., under seismic, flood and fire conditions), and root-causes that leave multiple components in inoperable states (e.g., due to maintenance errors), are excluded in this model. Nevertheless, nearly all CCF coupling factors [25] are influenced by component aging. That is, CCF events from all the environment-based coupling factors, including same component location and internal

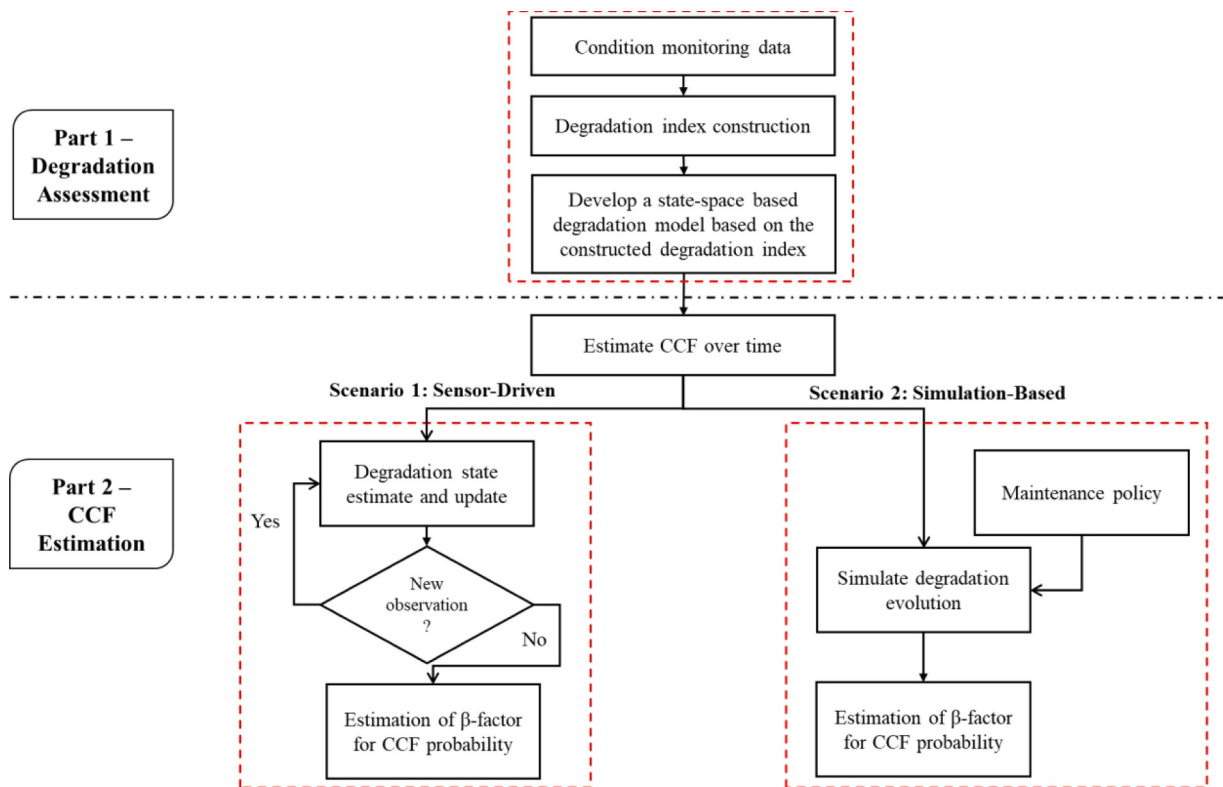


Fig. 2. Flowchart of the proposed approach.

environment/working medium, some of the operation-based coupling factors, such as same operating procedure and same maintenance/test/calibration, and some of the hardware-based coupling factors, such as component configuration and the attributes of manufacturing, construction and installation, can be attributed to age-related degradation.

To bridge the existing gaps and assumptions described earlier, this paper proposes a novel approach to modeling degradation-related CCF events by integrating the maintenance impacts and the component degradation evolution that can be characterized through condition monitoring data. The proposed approach consists of two main parts and adopts the CCF β -factor model without loss of generality. The first part focuses on the component degradation assessment. Specifically, the degradation state of each component is characterized through a degradation index obtained by extracting features of data obtained from sensors that monitor evidence of degradation. Based on the proposed degradation index, a state-space based degradation model is built to describe the component degradation evolution; this model considers the variations both within and across involved components. In the second part, the time-dependency of CCF events is estimated based on the detected degradation evolution. At each time instant, the β -factor for CCF probability is estimated as the fraction of the degradation states of multiple components that simultaneously exceed each component's endurance to degradation. The estimation of the β -factor for CCF probability, however, follows the conventional parametric CCF model. Accordingly, the scope of the parametric CCF model is dynamic over lifetime service rather than static. The component degradation evolution under imperfect maintenance and renewal is also simulated to support the CCF estimation over the lifetime. The maintenance effect on CCF is also investigated through sensitivity studies. The imperfect maintenance refers to situations where the maintenance restores a component to better than old, the same as old or worse than old conditions, but not to an "as good as new" condition.

The primary focus of this research is to advance the state-of-the-art CCF analysis by exploiting the opportunities provided by recent advances in sensor-based techniques that facilitate understanding of the

component degradation evolution [27,28]. Note that the terms *degradation state* and *degradation index* are used interchangeably in this paper, since the component degradation state is characterized by the proposed degradation index. The key elements of the proposed approach are summarized as follows:

- Integration of components' degradation evolutions to model CCF.
- Generalization of the common cause influences among similar or even slightly dissimilar components with shared features.
- Introduction of a new way to quantify the CCF.
- Infusion of physics-based information to the CCF.
- Reliance on a large amount of sensor-based condition monitoring data, to complement the scarcity of failure data.

The proposed approach is demonstrated below by a test rig generating diverse sensory data acquired from a special-purpose experiment involving a redundant pump system at the University of Maryland. Three centrifugal pumps were continuously tested, and the common cause dependencies were monitored and established through application of shared environment, identical system design and proximity. The pump conditions were monitored using three types of techniques including process monitoring, vibration monitoring, and acoustic emission (AE) monitoring. Development of pump failure analysis, degradation assessment and condition-based maintenance policy will also be presented in detail. Simulation, as well as sensitivity analysis, is performed to evaluate the effects of maintenance on CCF over the lifetime of components.

The remainder of this paper is organized as follows. Section 2 discusses the proposed approach to modeling CCF through integrating component degradation evolution. Section 3 presents the experimental design, instrumentation, pump failure analysis, degradation assessment, and CCF estimation results. Section 4 presents the conclusions.

2. Proposed approach

This section presents the proposed approach, which consists of two parts as illustrated by the flowchart in Fig. 2. Section 2.1 presents the modeling scope and some key assumptions, followed by a description of Part 1, the overall degradation assessment to CCF modeling. Section 2.2 covers treatment of the condition monitoring data, definition of the degradation index and development of the degradation model. Section 2.3 discusses Part 2, estimation of the β -factor for CCF probability.

2.1. Modeling scope and assumption

Before proceeding to the proposed approach, the modeling scope and some key assumption are summarized as follows:

- This research advances CCF analysis with a focus on multiple identical or similar components undergoing age-related degradation.
- Multiple components are operated under common conditions and environments.
- Components are equipped with condition monitoring capabilities, where the sensory data can be directly or indirectly correlated to the severity of the underlying degradation process.
- Effective degradation assessment methods are available to infer the degradation state for the components of interest.
- The component degradation evolution is modeled as a continuous process characterized by a physics-based model or a data-driven model.
- No maintenance-based rejuvenation is assumed in the development of sensor-driven scenario, which follows the state-of-the-art practice of degradation modeling.
- Effect of imperfect maintenance on CCF is accounted for by superimposing the amount of renewal achieved onto the estimation of the β -factor for CCF probability through simulation-based scenarios.

2.2. Degradation assessment

To accurately assess component degradation, three main steps must be taken: (1) determine the most useful condition monitoring techniques that would cost-effectively track component degradation state; (2) obtain useful degradation information that fully characterizes the underlying physical transition of degrading components; (3) develop an appropriate estimation model for the β -factor for CCF probability. In this section, the background of each step is briefly presented, and the main discussions focus on the methods specifically developed for the experimental study in Section 3.

2.2.1. Condition monitoring techniques

Condition monitoring techniques have been widely used to understand and track the component degradation [29]. A variety of techniques can be applied depending on the specific types of component and application of interest [30]. The sensor measurements collected using condition monitoring techniques are known as condition monitoring data, which are analyzed, trended and used to obtain indications of component degradation state. Note that baseline data should be collected usually in the pre-service period; these data provide information on initial component condition and provide a basis for comparison with the data from subsequent examinations [31]. Three typical condition monitoring techniques involved in this study are as follows:

- Process monitoring is a condition monitoring technique to detect problems by monitoring changes in any combination of the process variables such as pressure, temperature and power consumption. Monitoring the trend over a long period can typically provide indications of improper machine conditions.

- Vibration monitoring is the most common non-destructive technique to measure the level of vibration as acceleration, velocity or displacement. The level of vibration can then be compared to historical baseline values to assess the component's condition.
- AE monitoring was originally developed for non-destructive testing of static structures and has recently received a lot of attention for the applications to machinery condition monitoring. It offers the advantage of early fault detection in comparison to vibration monitoring due to the increased sensitivity of AE [30].

2.2.2. Degradation index construction

Degradation index construction is influenced by the nature of the data available. In general, the condition monitoring data [32] may be classified into two categories: (a) direct condition monitoring data that can be directly related to the underlying physics-of-failure, such as crack size measurements or amount of wear or corroded materials in the oil; (b) indirect condition monitoring data from which the degradation state can only be indirectly inferred, such as vibration and oil analysis data. With the growing complexity of engineered components, it is difficult or even impossible to identify the physical signals that directly characterize the underlying degradation process [33]. Typically, the raw signals are transformed into more informative features, so as to enhance the data quality to better represent the current component condition. As such, indirect approaches are more practical. Numerous signal processing methods are available to extract these features, including time-domain analysis, frequency-domain analysis, and time-frequency-domain analysis [34]. Then the fault relevant features need to be identified, and an appropriate transformation process is used to construct the degradation index. This transformation process is typically achieved by the common algorithms within five categories [35]: classification-based, statistical-hypothesis-testing-based, weighted-based, regression-based and distance-based methods. More recently, machine learning techniques have attracted attention, including application of deep learning to automatically identify data features for diagnostic and prognostic purposes [36].

In this paper, a distance-based degradation index is defined and used to characterize the degradation evolution observed during the experimental case study. Fig. 3 summarizes the basic steps necessary to assess the component degradation. The first step is to process the raw condition monitoring data to extract useful features that appropriately characterize the component condition. Then the anomaly is detected based on the distance between the test data formed by the features describing the current component condition and the training data observed during the normal operation. Specifically, in this approach, the distance is computed using the Mahalanobis distance (MD) methodology [37–39], which is a process of distinguishing multivariable data groups using a univariate distance measure. The magnitude of the MD values signifies the number of abnormalities, which can then be used to construct the degradation index indicating the component degradation state as a function of time.

Suppose the component condition can be described by an m -dimensional feature vector extracted from the raw condition monitoring data at each time step. The feature vectors as the training data collected at the i^{th} time step during the normal operation are denoted as $H_i = [h_{i1}, \dots, h_{ij}, \dots, h_{im}]$, where h_{ij} is the j^{th} feature observed at the i^{th} time step, with $i = 1, 2, \dots, n$ and $j = 1, 2, \dots, m$. Note that the i^{th} time step is the time index for the training data collected from the normal operation period. These training data are used to describe the normal operation by calculating the corresponding mean \bar{h}_j and standard deviation s_j of the j^{th} feature. Then normalize each feature of the training data as shown in Eq. (1):

$$h'_{ij} = \frac{h_{ij} - \bar{h}_j}{s_j}, \quad i = 1, 2, \dots, n, \quad j = 1, 2, \dots, m \quad (1)$$

where h'_{ij} is the normalized value of h_{ij} , $\bar{h}_j = \frac{1}{n} \sum_{i=1}^n h_{ij}$ and

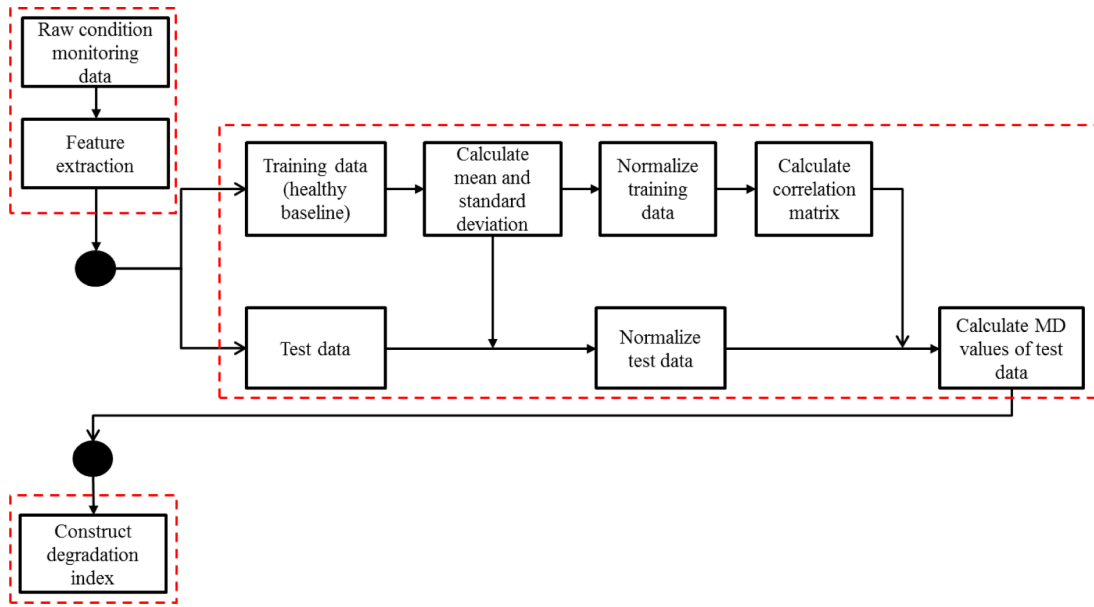


Fig. 3. Proposed degradation assessment method.

$s_j = \sqrt{\frac{\sum_{i=1}^n (h_{ij} - \bar{h}_j)^2}{n-1}}$. The normalized feature vector is denoted by $H'_i = [h'_{i1}, \dots, h'_{ij}, \dots, h'_{im}]$. The $m \times m$ covariance coefficient matrix, C , for the normalized vector H'_i in Eq. (2) would be:

$$C = \frac{1}{n-1} \sum_{i=1}^n H'_i{}^T \cdot H'_i \quad (2)$$

Consider the feature vectors as the test data collected during the abnormal operation, $F_k = [f_{k1}, \dots, f_{kj}, \dots, f_{km}]$, where f_{kj} is the j^{th} feature observed at the k^{th} time step, $k = 1, 2, \dots$, and $j = 1, 2, \dots, m$. Then obtain the normalized feature vectors F'_k of test data at the k^{th} time step by subtracting the mean \bar{h}_j and dividing by the standard deviation s_j . The MD value of the test data is calculated using the normalized vector F'_k and the covariance coefficient matrix C from Eq. (2):

$$M_k = \frac{1}{m} F'_k{}^T C^{-1} F'_k \quad (3)$$

where M_k is the MD value, F'_k is the normalized feature vector of the test data F_k , $F'_k{}^T$ is the transpose of the row vector F'_k , and C^{-1} is the inverse of the correlation matrix C ,

The MD values usually fluctuate since the degradation process is driven by multiple dependent competing failure mechanisms involving gradual degradation and random shocks. Post-processing (e.g., smoothing and filtering techniques) is usually required to obtain a smooth degradation index to track the component degradation. In this study, a distanced-based degradation index is proposed in Eq. (4) to extract the central tendency of the degradation, where Y_k is the degradation state at the time step k , and γ is a tuning parameter to control the extent of smoothing.

$$Y_K = \frac{\sum_1^k \log(M_k)}{k + \gamma} \quad (4)$$

2.2.3. State-space based degradation model

The degradation evolution of the s^{th} component $Y^s = \{Y_1^s, Y_2^s, \dots, Y_k^s\}$ is modeled as a continuous stochastic process, where Y_k^s is the degradation state of the s^{th} component at the time step k . Note that this process can be built according to a physics-based degradation model or some functional form referred to as the empirical degradation model based on the degradation index developed in Section 2.2.2. In this study, the degradation process is modeled by one of the most common stochastic

processes referred to as general path model [40]. The parametric function is assumed to be $Y_k^s = f(k; X_k^s, \varphi)$, where X_k^s is a vector of model parameters that is usually treated as a vector of random variables to account for unit-to-unit variability, and φ is an independent and identically distributed (i.i.d.) random error term. Herein, we assume the initial degradation state is zero without loss of generality. Note that this functional form can be linear, polynomial or exponential, and depends on the specific application. Furthermore, a state-space model is built to describe the dynamics of the degradation process, because of its ability to account for different sources of uncertainties [41–43]. The state-space model assumes that the degradation model parameters are unobserved states that evolve over time as a random walk process, so as to capture the variability across components. The variation within each component itself is reflected by the observation noise. The state-space model is applied to track the nonlinear degradation process of the s^{th} component in terms of the state function in Eq. (5) and observation function in Eq. (6).

$$\text{Statefunction: } X_k^s = X_{k-1}^s + V \rightarrow p(X_k^s | X_{k-1}^s) \quad (5)$$

$$\text{Observationfunction: } Y_k^s = f(k; X_k^s, \varphi) \rightarrow p(y_k^s | X_k^s) \quad (6)$$

where $f(k; X_k^s, \varphi_k)$ is the empirical degradation model, X_k^s is the state vector of the s^{th} component that is assumed as the hidden Markov process; Y_k^s is the observation (i.e., degradation index) of the s^{th} component that is conditionally independent given the hidden process; V_s is the i.i.d. process noise vector; φ is the i.i.d. observation noise; k is the time step; $p(X_k^s | X_{k-1}^s)$ is the transition distribution; and $p(Y_k^s | X_k^s)$ is the observation distribution.

2.3. Estimation of the β -factor for CCF probability

In the context of degradation modeling, a component failure is usually defined as the point at which the degradation state exceeds a predetermined level of endurance to degradation. Given that the degradation state estimate is known at each time instant, the occurrence of CCF would be indicated by the concurrent exceedance of the endurance to degradation. Therefore, the CCF impacts would be characterized by the fraction of multiple exceedances of the endurance to degradation, which follows the conventional parametric CCF model. As such, the scope of the parametric CCF model would be extended to be dynamic over the service lifetime rather than being static. Interested readers are directed to Reference 28 for more discussions on extending

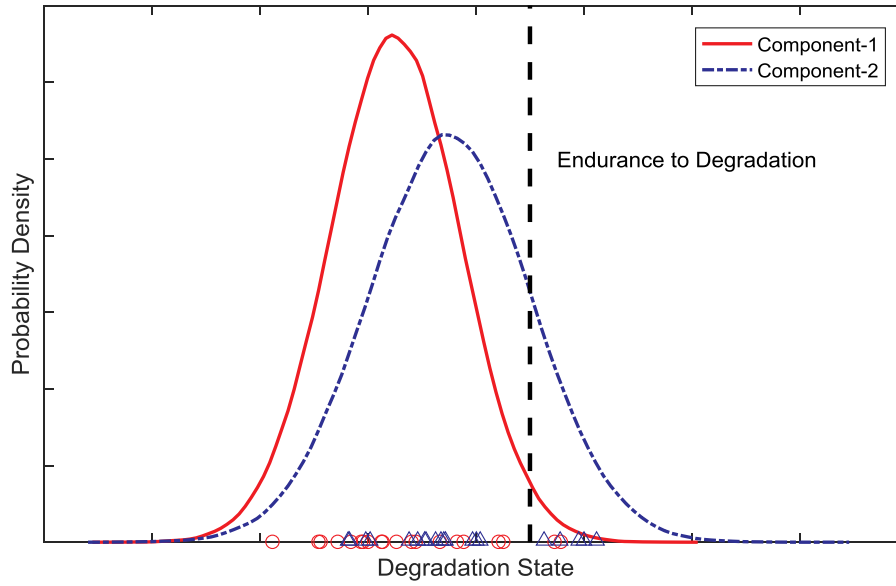


Fig. 4. Characterization of CCF with the components' degradation states and endurance to degradation.

risk assessment using degradation states estimated from condition monitoring.

Without loss of generality, as illustrated in Fig. 4, suppose the degradation state of component 1 is realized by the N samples $x_{1:N}^{(1,k)}$ denoted by circles and the degradation state of component 2 is realized by the N samples $x_{1:N}^{(2,k)}$ denoted by triangles at the time step k . The endurance to degradation L_f is treated as the same for both components, as is the convention of CCF. Note that it is straightforward to generalize to different points of endurance to degradation regarding each component due to the different operational requirement. Also, knowing the components' degradation provides the basis to conduct reliability analysis [33,40], for instance, the failure probability of a pump is calculated as the fraction of the samples beyond the endurance to degradation as displayed in Fig. 4.

All the samples associated with each component at each time step would be gathered to describe the degradation state of the two-component system. In this study, the β -factor model is adopted for demonstration, where the β -factor is defined as the fraction of dependent failures at each instant of time that involves multiple components. Specifically, the β -factor at each time instant k is estimated as the fraction of dependent failures involving more than a single component as represented in Eq. (7), where the denominator denotes the number of all failures and the numerator denotes the number of dependent failures:

$$\beta_k = \frac{\sum_{j=1}^N \{ \prod_{s=1}^M I(x_k^{(s,j)}, L_f) \}}{\sum_{j=1}^N \{ \prod_{s=1}^M I(x_k^{(s,j)}, L_f) \}} \quad (7)$$

$s = 1, \dots, M; j = 1, \dots, N.$

where, β_k is the estimate of the degradation CCF β -factor parameter at the time step k , L_f denotes the endurance to degradation, N is the total number of samples, M is the total number of components, $x_k^{(s,1:N)}$ is the realization of the degradation state of component s at the time step k , $I(a, b)$ is the state indicator function, which is 1 when $a > b$, and otherwise equals 0.

2.3.1. Sensor-driven degradation monitoring

Sensor-driven monitoring enables the β -factor for CCF probability to be estimated by combining the general degradation property with the sensor monitoring data of plant-specific components. To do this, we monitor individual components using real-time sensor monitoring data to update the component degradation states, and in turn, update the CCF estimation. Specifically, the state-space model in Section 2.2.3 is

further utilized such that once the sensor monitoring data are collected from an operating component, the hidden states can be inferred to calibrate the estimate of CCF in real time. The recursive Bayesian updating method provides a rigorous and general way to estimate the posterior probability density function (pdf) of the degradation state of the s^{th} component $p(\mathbf{X}_k^s | \mathbf{Y}_{1:k}^s)$ given the observations. Through recursive Bayesian filtering, prediction and update will be recursively implemented in two steps.

- (1) Prediction step: obtain the prior pdf $p(\mathbf{X}_k^s | \mathbf{Y}_{1:k-1}^s)$, which means that the state \mathbf{X}_k^s is inferred from the observations $\mathbf{Y}_{1:k-1}^s$.

$$p(\mathbf{X}_k^s | \mathbf{Y}_{1:k-1}^s) = \int p(\mathbf{X}_k^s | \mathbf{X}_{k-1}^s) p(\mathbf{X}_{k-1}^s | \mathbf{Y}_{1:k-1}^s) d\mathbf{X}_{k-1}^s \quad (8)$$

- (2) Update step: obtain the posterior pdf $p(\mathbf{X}_k^s | \mathbf{Y}_{1:k}^s)$ in terms of the current observation.

$$\begin{aligned} p(\mathbf{X}_k^s | \mathbf{Y}_{1:k}^s) &= \frac{p(\mathbf{X}_k^s | \mathbf{Y}_{1:k-1}^s) p(\mathbf{Y}_k^s | \mathbf{X}_k^s)}{p(\mathbf{Y}_k^s | \mathbf{Y}_{1:k-1}^s)} \\ &= \frac{p(\mathbf{Y}_k^s | \mathbf{X}_k^s) \int p(\mathbf{X}_k^s | \mathbf{X}_{k-1}^s) p(\mathbf{X}_{k-1}^s | \mathbf{Y}_{1:k-1}^s) d\mathbf{X}_{k-1}^s}{\iint p(\mathbf{Y}_k^s | \mathbf{X}_k^s) p(\mathbf{X}_k^s | \mathbf{X}_{k-1}^s) p(\mathbf{X}_{k-1}^s | \mathbf{Y}_{1:k-1}^s) d\mathbf{X}_{k-1}^s d\mathbf{X}_k^s} \end{aligned} \quad (9)$$

It is usually difficult to obtain Eq. (9) in a closed form, so we must resort to Monte Carlo methods. In this study, the particle filtering approach is used to achieve such a recursive state estimate and update because of its capability of handling non-linear and non-Gaussian systems. The key idea of particle filter [44] is to approximate the posterior pdf $p(\mathbf{X}_k^s | \mathbf{Y}_{1:k}^s)$ at the k^{th} step by N random samples or particles $\{\mathbf{X}_k^{(s,j)}\}$ with associated weights $\{\omega_k^{(s,j)}\}$, $j = 1, \dots, N$. Here N is the total number of particles:

$$p(\mathbf{X}_k^s | \mathbf{Y}_{1:k}^s) \approx \sum_{j=1}^N \omega_k^{(s,j)} \delta(\mathbf{X}_k^s - \mathbf{X}_k^{(s,j)}) \quad (10)$$

where δ is Dirac's delta function and $\omega_k^{(s,j)}$ is the weight of the j^{th} particle of the s^{th} component at time k .

The weights are normalized as $\sum_i^N \omega_k^{(s,i)} = \mathbf{I}$, where \mathbf{I} is the identity column vector. The sample $\mathbf{X}_k^{(s,j)}$ is drawn from importance density $q(\mathbf{X}_k^{(s)} | \mathbf{Y}_{1:k}^s)$. Through recursive relation, the weights are updated as

follows:

$$\omega_k^{(s,j)} \propto \frac{p(Y_k^s | X_k^{(s,j)}) p(X_k^{(s,j)} | X_k^{(s,j-1)})}{q(X_k^{(s,j)} | X_{k-1}^{(s,j)}, Y_{1:k}^s)} \cdot \omega_{k-1}^{(s,j)} \quad (11)$$

After multiple iterations, the variance of the weights increases such that only some particles have a significant weight, and all the other particles have negligible weights. This is known as the degeneracy problem, which is usually addressed by a resampling to eliminate particles that have small weights and concentrates on particles with large weights [45]. At each time step, the samples obtained from the resampling process could be viewed as the realizations of the degradation state for each component, and hence can be used to estimate CCF as shown in Eq. (7).

2.3.2. Consideration of maintenance impacts on degradation-based common cause failure probability

This section aims to develop a simulation-based approach to superimpose the imperfect maintenance on the degradation process identified in Section 2.2. The component degradation history can then be simulated given the identified component degradation process and the specific maintenance policy. With a few iterations of simulations, one can generate samples of component degradation states at each time step which are ultimately used to estimate the β -factor as shown in Eq. (7). This allows the effects of various maintenance policies on the CCF potential over the component lifetime to be evaluated.

A generic condition-based maintenance policy is established for elucidating the approach. The maintenance policy is subject to the following assumptions (the authors also recognize the possibility of optimizing the decision variable [46,47], which is out of the scope of this paper). Note that the maintenance mode is general and could be customized according to the application of interest, such as adjusting the inter-inspection interval and repair quality.

- The component is subject to periodic inspection, and the component failure can only be detected at the time of inspection.
- The inspection itself is perfect in that it reveals the true degradation state of the component and does not change the condition of the component.
- Inspection and maintenance actions take negligible time compared to the expected lifetime of the maintained component.
- Preventive and corrective replacement is perfect, while preventive maintenance (PM) could be imperfect.
- Each component over lifetime service would randomly follow one of the various types of classical degradation processes or failure mechanisms according to the knowledge of component's historical performance.

Suppose the inter-inspection interval length is ΔT , so the degradation state of a component after its installation at time 0 will be inspected and measured at times $\{T_i = i\Delta T; i = 1, 2, \dots\}$. According to the degradation state Y_{T_i} at the i^{th} inspection, one of the following maintenance actions would be needed, and the degradation state of the component after maintenance would be $Y_{T_i}^*$:

- If $Y_{T_i} \leq L_r$, no maintenance action is performed, and $Y_{T_i}^* = Y_{T_i}$, where L_r is the preventive repair threshold.
- If $L_r < Y_{T_i} \leq L_p$, an imperfect preventive maintenance of the component is immediately performed. The impact of imperfect maintenance is considered by adjusting the degradation state of a maintained component by a random amount to some level lower or equal to the preventive repair threshold L_r . As such, $Y_{T_i}^*$ would be $(1 - \theta) \cdot L_r$, where θ is a rejuvenation factor defined within the interval $[0, 1]$. The θ indicates the degree of repair and follows the beta distribution parameterized by two positive shape parameters, denoted by α and γ . Note $\theta = 1$ means a perfect repair and $\theta = 0$

means a minimal repair, and L_p is the preventive replacement threshold.

- If $L_p < Y_{T_i} \leq L_f$, preventively replace the system. In doing so, the component is considered as good as new, which means $Y_{T_i}^*$ is equal to zero, and L_f is the threshold (i.e., endurance to degradation) to trigger corrective replacement.
- If $Y_{T_i} \geq L_f$, the component fails and correctively replace the component. The component is considered as good as new, indicating $Y_{T_i}^*$ equals to zero.

3. Experimental study

There are six steps involved in the experimental case study to demonstrate the proposed approach: (1) design a special-purpose experiment with advanced sensing capabilities for a redundant pump system; (2) conduct failure analysis to identify the failure mechanisms and root causes; (3) construct a degradation index using information from diverse sensor data; (4) develop a degradation model that quantitatively characterizes the degradation evolution; (5) estimate the β -factor for CCF probability using the observed sensor monitoring data; (6) estimate the β -factor for CCF probability by simulating, superimposing and accounting for the inspection frequency and the rejuvenation effects of preventive maintenance.

3.1. Experimental design and instrumentation

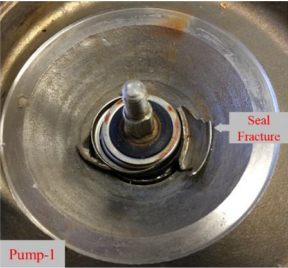
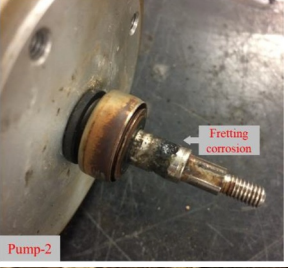
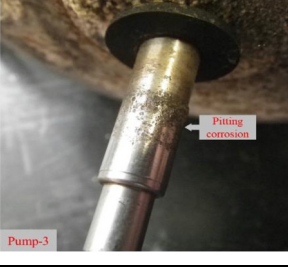
As an active component susceptible to CCF [48], the centrifugal pump was chosen for this case study to demonstrate and validate the proposed approach. The general-purpose horizontal centrifugal pump tested was a mechanically sealed pump driven by a 12-Vdc Totally Enclosed Fan-Cooled (TEFC) motor. The centrifugal pumps were tested from brand-new condition to full failure inside a temperature chamber at around 70 °C, where pump were exposed to recirculated seawater at elevated temperature around 75 °C, whereby accelerating degradation, aging and eventual failure. Accordingly, the common-cause dependencies among the pumps were rooted in the same component configuration, the same operating practice, and common inter-environmental conditions (i.e., elevated temperature) and intra-environmental conditions (i.e., elevated temperature and corrosive seawater).

Unlike most current research based on the data acquired from artificially-seeded damage experiments, no artificial damage was seeded in this experimental setting, to more closely represent the real field situation. Since the useful life of a centrifugal pump can range from several months to a few years, the experiment was planned to stop when the pump fully or partially ceased to perform.

The operating conditions of the pumps tested were continually monitored by the sensing system, which comprises three types of condition monitoring techniques:

- 1 *Process monitoring* was implemented through measurements of the pump's differential pressure, flow rate, electric current and electric voltage. All the measurements were performed at the sampling rate of 0.5 Hz using a Keysight Technology 34972A LXI data acquisition and an in-house developed Labview-based tool.
- 2 *Vibration monitoring* was implemented using three single-axis AC240 accelerometers from Connection Technology Center (CTC) Inc., the National Instruments (NI)-9230 analog input module, NI-cDAQ-9174 CompactDAQ chassis, and an in-house developed Labview-based tool. To ensure accurate measurement, the sampling rate was set at 10,240 Hz, which is approximately 40 times the maximum vane passing frequency. The recordings of every 60 s of data were stored in a separate file.
- 3 *AE monitoring* was implemented using three Micro30 miniature AE sensors manufactured by Physical Acoustics Corporation (PAC). The sensors were placed in three locations on the pump: suction, bearing, and motor. The sampling rate was set at 1 MHz. The output

Table 1
Failure analysis for each of the three pumps.

Index	Failure observation	Duration	Failure mode	Failure mechanism	Root cause
Pump 1		1954 h	Seal fracture	Fatigue	Excessive fluid pressure on seal caused seal fracture. The broken pieces then led to rubbing between pump's housing and impeller, which caused the impeller to stick, and the pump functionally stopped.
Pump 2		5103 h	Corrosion	Fretting corrosion	Fretting corrosion occurred on the contact surface between the mechanical seal and the rotating shaft. This caused extensive corrosion indicated by the red-brown corrosive fluid.
Pump 3		4654 h	Pump leaking	Pitting corrosion	Pitting corrosion occurred on the contact surface between the mechanical seal and the rotating shaft. This caused serious leakage located in the coupling section.

signal was pre-amplified at 40 dB and was collected by a commercial AE data acquisition System by PAC. The AE signals from all three channels were recorded simultaneously by extracting selected features such as absolute energy, root mean square (RMS), and counts.

3.2. Pump failure analysis

The interactions between the surrounding environment and the operating pump could lead to degradation in form of changes in physical properties and dynamic behaviors including part damage and reduction of performance. Failure analysis was conducted after the experiment to identify the root causes and the actual failed parts of the pumps. Table 1 shows the experiment duration, failure mode and failure mechanism and root causes for each pump. The pumps are subject to three different general aging failure mechanisms of fatigue, fretting corrosion and pitting corrosion.

3.3. Pump degradation assessment

This section describes the construction of the degradation index based on the three types of condition monitoring data. The main challenge was to extract useful information from raw sensor signals and to establish a feature vector representing the pump condition. The degradation assessment method proposed in Section 2.2.2 was used to construct a degradation index using the established feature vector with the tuning parameter $\gamma = 100$. Data collected in the first ten days of the testing were used to establish the health baseline that characterizes the pump's normal operation.

3.3.1. Process monitoring data

The pump degradation state was monitored by the rich information contained in the pump efficiency data derived from the four measured operational characteristics: electric current, electric voltage, differential pressure and flow rate. The objective was to track the statistical features extracted from the pump efficiency data that indicate the pump performance fluctuations as it degraded. As shown in Eq. (12), the pump efficiency η is determined as the ratio of the hydraulic power P_h to the electric power P_e consumed by the pump [49]:

$$\eta = \frac{P_h}{P_e} = \frac{Q \cdot \rho \cdot g \cdot H}{U \cdot I} \quad (12)$$

where U is the electric voltage, I is the electric current, ρ is the density of the pump liquid, g is the gravity constant, Q is the measured flow rate, and H is the pump head converted from the measured differential pressure [49].

The four sensor measurements were first smoothed with a moving average filter and then used to determine the pump efficiency according to Eq. (12). The pump efficiency data were segmented every hour, and various statistical features were extracted from each segment. Specifically, seven statistical features were extracted that represent the energy and shape of the distribution of the pump efficiency data, including mean value, peak to peak value, root mean square, standard deviation, crest factor, shape factor and mean square frequency. These features constituted a seven-dimensional feature vector describing the pump operating condition. The resulting degradation index of the three pumps is illustrated in Fig. 5, where the x-axis is the testing time of pumps and the y-axis is the degradation index. The same pattern in the degradation index was observed indicating similar degradation paths for all pumps.

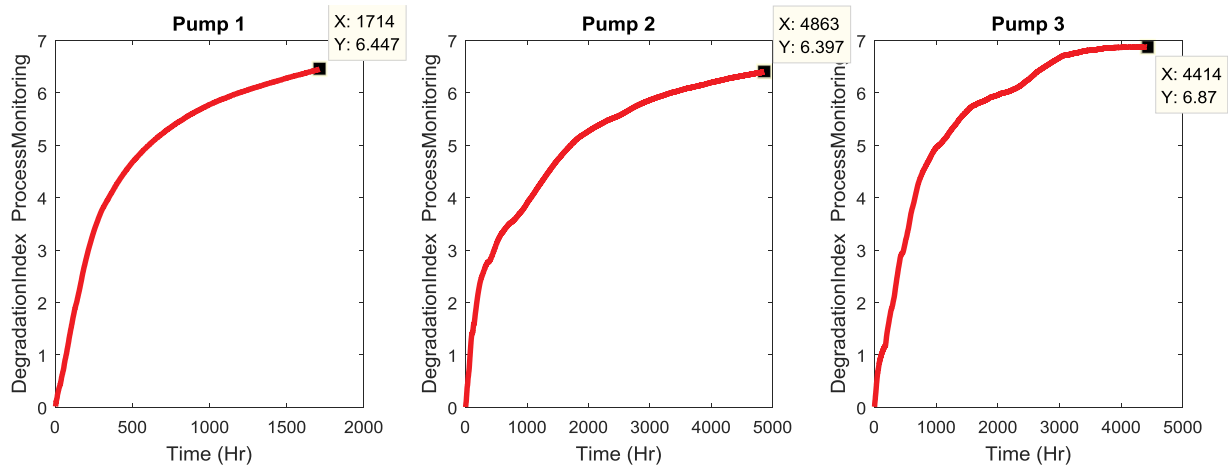


Fig. 5. Degradation index constructed based on process monitoring data.

3.3.2. Vibration monitoring data

The operating pumps produce vibration signals with distinctive characteristics recognized by specific vibration spectrum patterns [50]. By inspecting the frequency spectrum of the related vibration signals, one can identify the characteristic frequencies, tracking the changes that uniquely indicate pump degradation status.

In this study, the vibration signals were segmented every minute, and then each segment was transformed into a frequency spectrum using Fast Fourier transform (FFT). The first step was to identify the characteristic frequencies by searching for the frequencies with top one-hundred magnitudes in the frequency spectrum. The measurements collected from all three directions were analyzed to explore the allocation of energy within the frequency spectrums. The same pattern was discovered in each pump: most energy was distributed in the five principal frequency bands from 20 Hz to 300 Hz. Indeed, variations existed across different pumps because of the speed variations and the different failure mechanisms involved. The next step was to track the pump condition by measuring the energy of characteristic frequencies, which is expressed by the RMS of the spectrum magnitude in terms of the five principal frequency bands. Given one single-axis vibration signal at each time instant, the pump condition could be represented by a five-dimensional feature vector consisting of the RMS of each characteristic frequency. In this study, the vibration data from the three directions were used to establish a fifteen-dimensional feature vector to describe the pump condition at each time step. Fig. 6 demonstrates the degradation index for the three pumps. It is important to note the similar pattern observed among the three pumps' degradation paths.

3.3.3. AE monitoring data

The sources of AE in rotating machinery include impacting, friction, turbulence, cavitation and leakage [51]. Depending on the underlying failure mechanism, the degradation of a rotating machine can be captured by the changes in the AE signal features (e.g., amplitude, counts, energy), among which the energy-related features are useful indicators of damage in rotating machinery [52]. The energy-related features include RMS, energy, absolute energy and average signal level.

In this study, it was observed that all four types of energy-related features above were highly correlated, and hence only the RMS feature was selected for further analysis. The RMS features were utilized in terms of the AE signals collected in each of the three different locations. Thereafter, a three-dimensional feature vector was established to describe the pump condition at each time step. Fig. 7 shows the degradation index of the three pumps, where the x-axis is the testing time of pumps (in hours), and the y-axis is the magnitude of degradation index. The results also show a similar pattern across different pumps.

3.4. Pump degradation model development

Given the three types of degradation indices constructed in Section 3.3, this section first discusses the most appropriate degradation index that can be used to characterize the degradation behaviors of the three pumps, followed by a description of a state-space based degradation model.

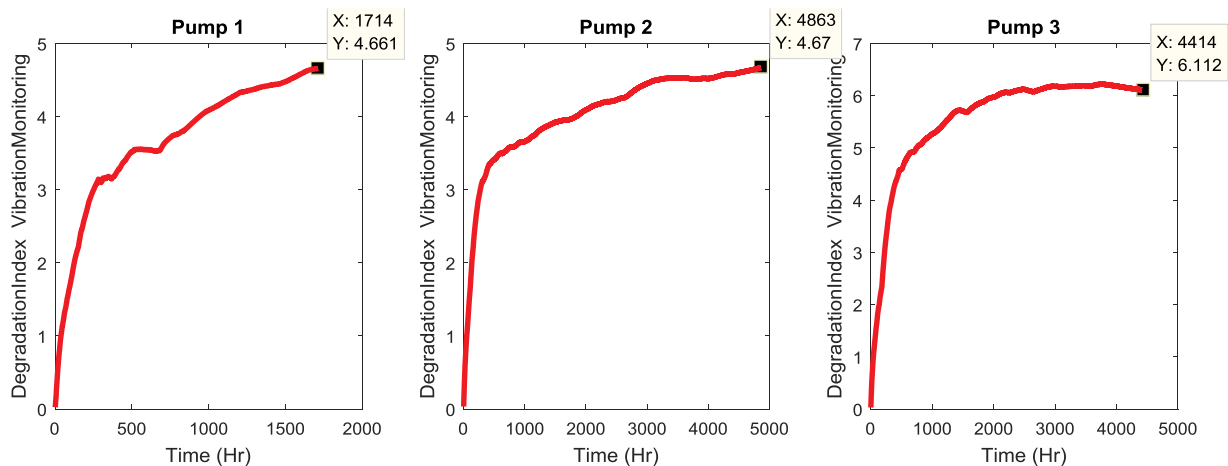


Fig. 6. Degradation index constructed based on vibration monitoring data.

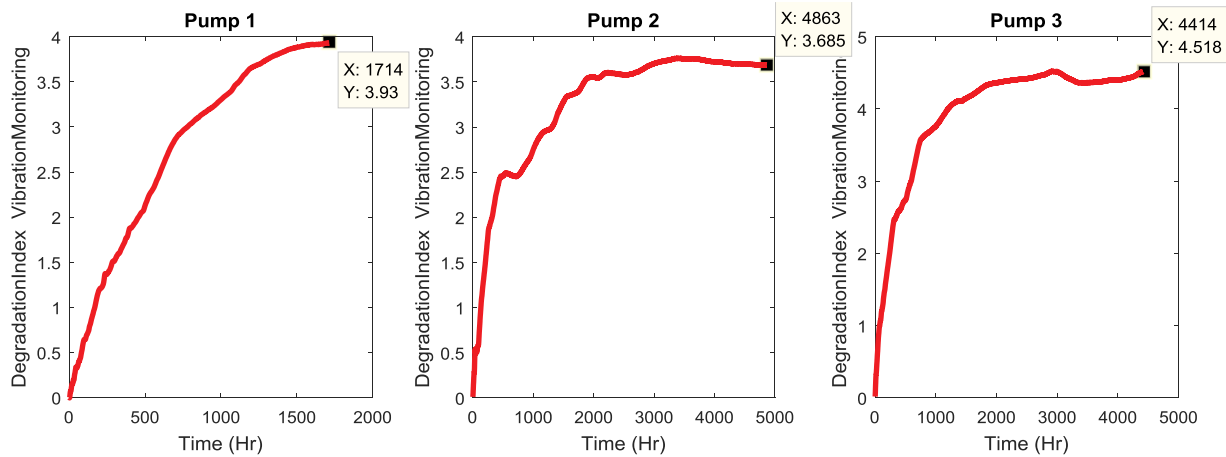


Fig. 7. Degradation index constructed based on AE monitoring data.

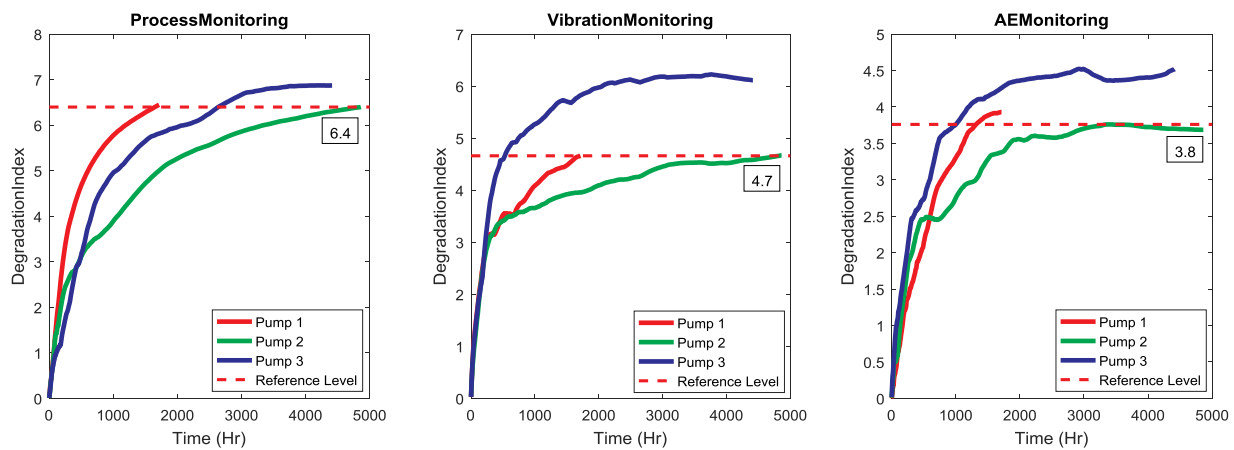


Fig. 8. Degradation index regarding three types of condition monitoring data.

3.4.1. Selection of degradation index

The degradation profiles of the three pumps are summarized in Fig. 8 for each type of condition monitoring technique used. For comparison purposes, a reference level is provided of the minimum value of the degradation index at the end of each experiment. It clearly shows that the degradation profiles of the pumps tend to be highly correlated in all three types of condition monitoring technique. On the other hand, regardless of the sensitivity or sampling frequency differences among the monitoring techniques, the same functional relationship could be applied to characterize the pump degradation behaviors associated with different failure mechanisms. Indeed, the ability to track the pump degradation behavior varied depending on the sensitivity of condition monitoring technique to the underlying failure mechanism. Some insights are summarized as follows:

- For all three monitoring techniques used in this study, the levels of degradation index tended to stabilize at the end of the test, which provides a reference level to properly define the endurance to degradation. Clearly, variations exist due to the stochastic nature of the degradation process.
- Given the same failure mechanism, the sensitivity of the condition monitoring technique was different. Hence, the same family of monitoring technique should be used to monitor.
- Different failure mechanisms may have distinct influences on the degradation evolution, which can be indicated by the differences between degradation rate and/or degradation state. For instance, the failure mechanism underlying Pump 3 (pitting corrosion) results in a higher degradation state than those involved in Pump 1

(fatigue) and Pump 2 (fretting corrosion).

- The developed degradation index is demonstrated to be applicable to a pump involved in any one of the three failure mechanisms.

With the three types of degradation index, the most appropriate degradation index was related to the process monitoring data. This choice was based on the following criteria [53,54]: (a) the variance in the failure limit of the developed degradation index should be minimal; (b) the larger slope of the data provides a clearer trend; and (c) the range of information should be as large as possible. Indeed, the authors also recognize that a fusion approach has the potential to improve the characterization of the degradation evolution by making use of the information from different monitoring techniques, but this was considered out of the scope of this paper. Finally, the endurance to degradation should be selected as some value lower than the degradation state at the end of each test, where the pumps failed. Specifically, the endurance (or capacity) to degradation, L_f , was empirically selected as 6.0, which is lower than the reference level 6.4 to maintain a moderate safety margin.

3.4.2. Degradation model development

Once the degradation index was developed, a mathematical degradation model was needed to describe the pump degradation evolution. Examination of the degradation index showed that the degradation path follows the power function in Eq. (13):

$$y_k = a \times k^b + c + \varepsilon \tag{13}$$

where a, b and c are the model parameters, k is the time step, y_k is the

Table 2
Results for regression and goodness-of-fit statistics.

Component	Goodness-of-fit statistics			Model parameters		
	R^2	Adjusted R^2	RMSE	a	b	c
Pump 1	0.9763	0.9762	0.2386	5.206	0.1367	-7.711
Pump 2	0.9915	0.9915	0.1245	1.985	0.1908	-3.355
Pump 3	0.9644	0.9643	0.3054	7.47	0.1063	-10.94

observation of the degradation index at time step k , and ε is the additive Gaussian noise with zero means and different standard deviation σ . To demonstrate the feasibility of Eq. (13) for describing the degradation evolution, a nonlinear least squares regression is conducted for the selected degradation index. The goodness-of-fit statistics is employed to measure the fitting performance of Eq. (13). The R-squared values (R^2), the adjusted R^2 , the root mean squared error (RMSE) and model parameters are summarized in Table 2. Based on these results, one can conclude that Eq. (13) represents a good fit for describing the degradation evolution.

The pump state-space model used in this paper is constructed as follows. The power function is used as the observation function, and the model parameters are incorporated as the elements of the state vector with $s = 1, 2, 3$.

State Function:

$$a_k^s = a_{k-1}^s + \varepsilon_1 \quad (14)$$

$$b_k^s = b_{k-1}^s + \varepsilon_2 \quad (15)$$

$$c_k^s = c_{k-1}^s + \varepsilon_3 \quad (16)$$

Observation Function:

$$Y_k^s = a_k^s \times k^{b_k^s} + c_k^s + \varepsilon_4 \quad (17)$$

where k is the time step, Y_k^s is the observation of the degradation index of the s^{th} pump at time step k , a_k^s , b_k^s and c_k^s are the model parameters of the s^{th} pump at time step k , and ε_1 , ε_2 , ε_3 and ε_4 are the additive Gaussian noises with zero means and different standard deviation σ_1 , σ_2 , σ_3 and σ_4 , respectively.

3.5. Experimental results for CCF estimation

3.5.1. Results for sensor-driven scenario

As shown in Fig. 9, the entire testing profile is categorized into three phases (Phase 1, Phase 2 and Phase 3) based on the system configuration changes. Phase 1 involved a three-pump redundant system from

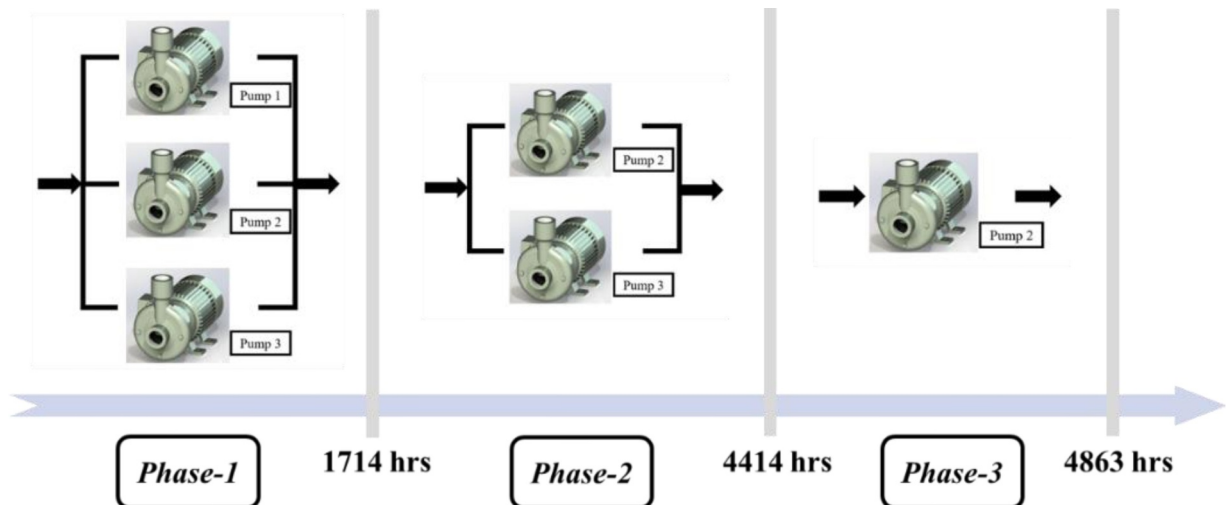


Fig. 9. Testing profile with three phases.

the beginning to 1714 h of operation. When Pump 1 failed, the test proceeded to Phase 2 involving a two-pump redundant system until 4414 h of operation. After Pump 3 failed, Phase 3 ran with only Pump 2 until 4863 h of operation. Note that only Phase 1 and Phase 2 are of interest for CCF events.

At a time instant of 1500 h of operation, the degradation state of each pump is estimated and characterized by six thousand samples as illustrated by the histograms in Fig. 10(a), which respectively indicates the number of occurrences for the possible degradation states associated with all three pumps. Then the CCF is estimated based on the fractions of concurrent exceedance of endurance to degradation as discussed in Section 2.3. Therefore, given newly arrived sensor monitoring data at each time instant, the degradation state of each pump is estimated and is then used to update the CCF estimation according to Eq. (7). Fig. 10(b) displays the estimate of CCF over the entire test, which shows the dynamic features of CCF assuming no maintenance-based rejuvenation.

According to Eq. (7), the CCF for Phase 1 and Phase 2 are estimated as displayed in Fig. 11. The differences between Phase 1 and Phase 2 are attributed to the different failure mechanisms underlying each pump and system configuration changes. Some important observations are summarized as follows:

- Over the entire test, the β -factor starts from zero and approaches one at the end. It is intuitive that the redundant pump system would fail eventually without any maintenance actions.
- In Phase 1, Pump 1 degrades much faster than the others, as is evident from its shortest experiment duration in Section 3.2. As such, Pump 1 is subject to more likely failure, while the other two pumps are not. It appears that independent failure is dominant in Phase 1, which results in low β -factor.
- In Phase 2, the β -factor approaches one because of the pump degradation without mitigating actions.
- From the perspective of the CCF control, knowing the pump degradation state allows one to determine the time required to implement mitigating actions based on some critical level of CCF [55]. Suppose the β -factor should be less than 0.05, as such maintenance actions would be needed before 2870 h of operation.

3.5.2. Results for simulation-based scenario

With the knowledge of the degradation processes involved in the three testing pumps, a condition-based maintenance policy was selected as illustrated in Fig. 12(a). It is assumed that the preventive repair threshold is $L_r = 4$, the preventive replacement threshold is $L_p = 5$, and the endurance to degradation is $L_f = 6$. During service, the pump is

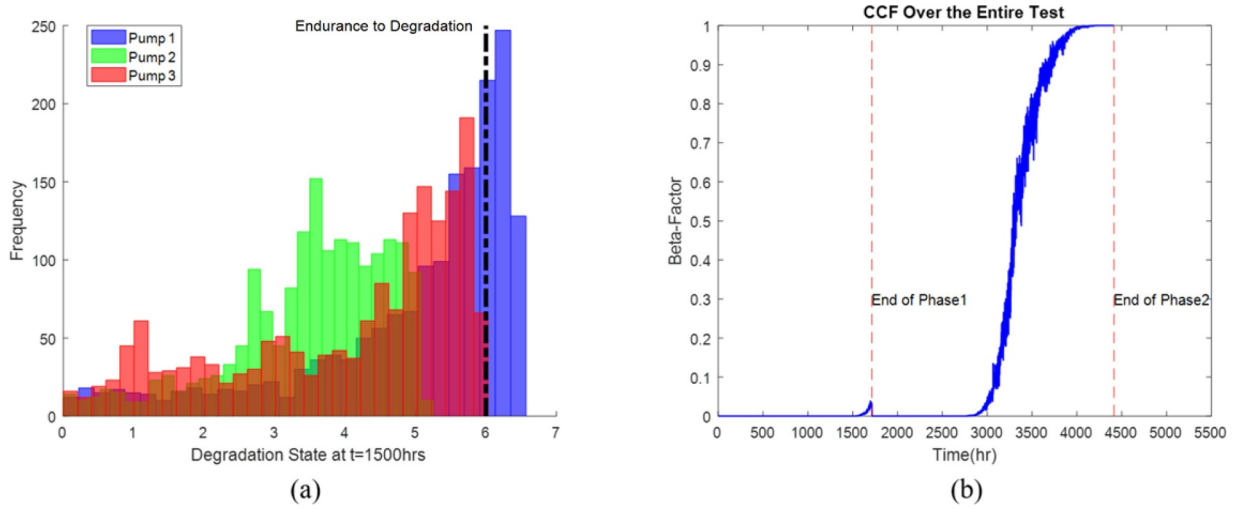


Fig. 10. (a) Illustration of the degradation states of all three pumps at $t = 1500$ h; (b) estimate of the β -factor over the entire test (note that no renewal involves so the β -factor theoretically reaches unity).

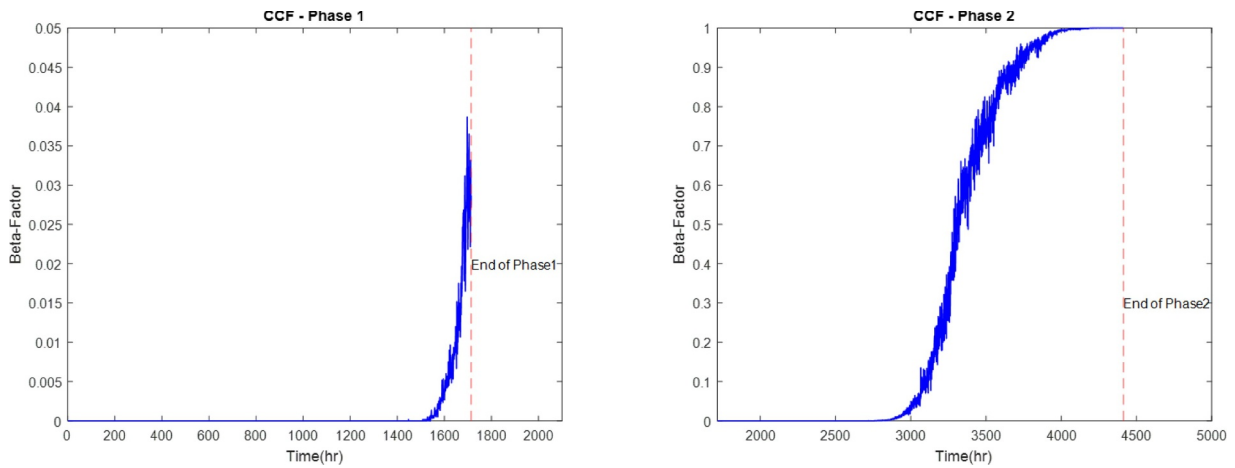


Fig. 11. Estimate of the β -factor for Phase 1 and Phase 2 (involving no renewal that rejuvenates the components).

subject to any of the three failure mechanisms identified in Section 3.2. The degradation behavior would be random throughout the service based on the different parameters set regarding the three failure mechanisms as provided in Table 2. The following results are generated

based on the simulation of one year of pump service.

As an illustrative example, suppose the inspection interval is $\Delta T = 720$ h, and the rejuvenation or renewal factor follows the beta distribution with $\alpha = 5$ and $\gamma = 1.5$, indicating good maintenance

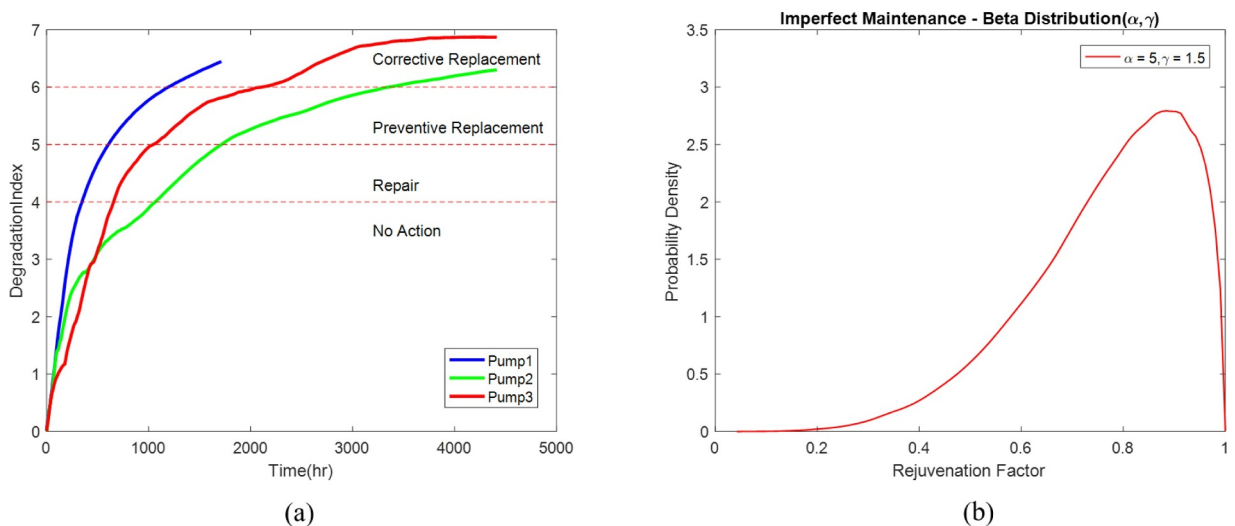


Fig. 12. (a) Condition-based maintenance policy; (b) imperfect maintenance characterized by the beta distribution with $\alpha = 5$ and $\gamma = 1.5$.

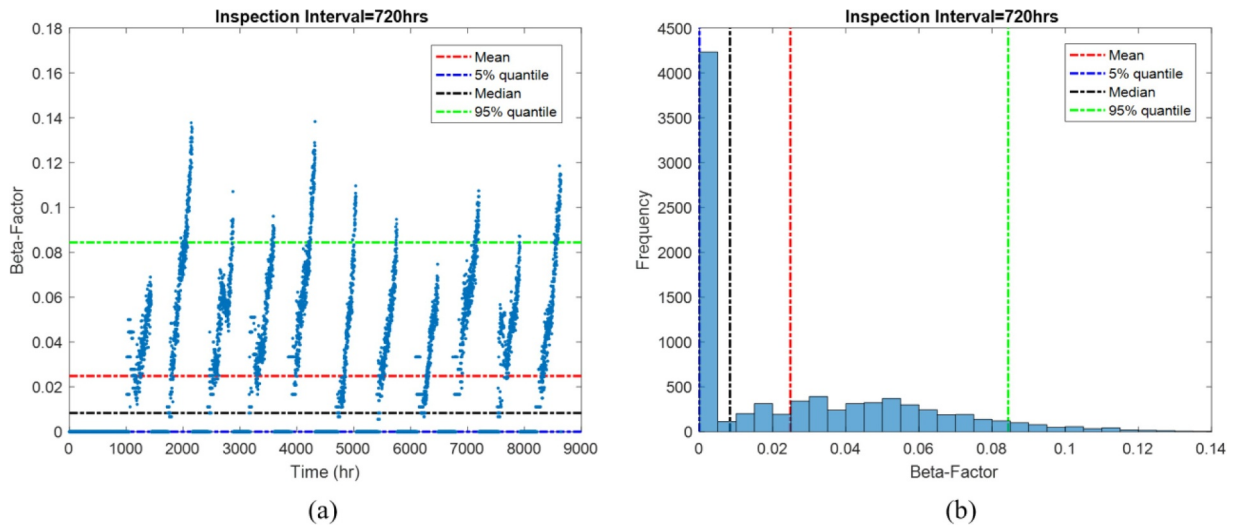


Fig. 13. (a) Hourly evolution of the β -factor; (b) distribution of the β -factor in relation to component degradation and maintenance actions.

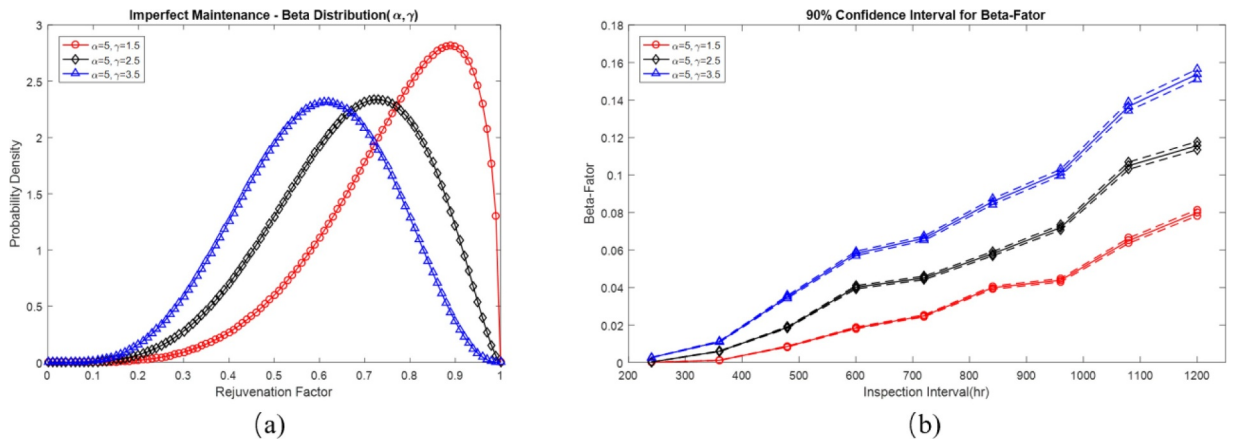


Fig. 14. (a) Three options for rejuvination factor considered in the sensitivity analysis; (b) 90% confidence interval for the β -factor according to twenty-seven imperfect maintenance policies.

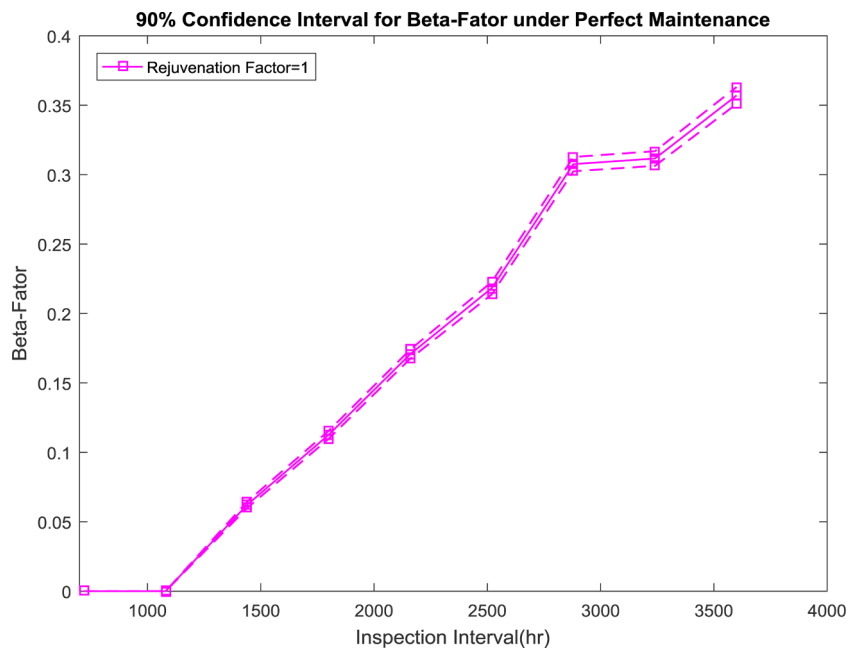


Fig. 15. 90% confidence interval for the β -factor according to nine perfect maintenance policies.

practices as displayed in Fig. 12(b). This is a typical scenario in practice where rejuvenation due to maintenance is imperfect. The hourly evolution of the β -factor is provided in Fig. 13(a), and the overall variability of the β -factor is summarized by the distribution of the β -factor as shown in Fig. 13(b). The mean estimate of the β -factor is 0.025, and the component failure rate is 4.1×10^{-4} failures/hr. The 5% quantile, median, and 95% quantile estimates of β -factor are 0, 0.008 and 0.084, respectively. Some important observations are discussed as follows:

- The dynamic characteristics of CCF are captured by evolution of the β -factor, which shows a periodical increasing trend. This indicates that the β -factor would be underestimated as the components degrade and maintenance actions vary, which results in the underestimation of plant risks.
- It is expected that most β -factors are close to zero, and the distribution of β -factor is positively skewed. The variation of β -factor is large and is attributed to the underlying component degradation and the relevant maintenance actions.
- Examination of the quantile estimates indicates that simply treating the CCF impacts based on the mean estimate of β -factor is not sufficient and would lead to underestimation of the β -factor.

Different maintenance policies lead to different patterns of β -factor through component service. Therefore, a sensitivity study was conducted to investigate the CCF changes under different maintenance effectiveness in terms of two decision parameters: the inspection interval ΔT and the rejuvenation factor θ . There are twenty-seven maintenance interval and effectiveness characteristics defined by the combinations of (1) nine options for inspection interval ΔT in units of hours: {240, 360, 480, 600, 720, 840, 960, 1080, 1200}, and (2) three options for rejuvenation factor with the parameter sets (α, γ) : {(5, 1.5), (5, 2.5), (5, 3.5)}, which respectively represents a decreased degree of repair as displayed in Fig. 14(a).

The results of the sensitivity analysis are summarized in Fig. 14(b), which provides the 90% confidence interval for the mean estimates of the β -factor for each imperfect maintenance characteristic. The results are used to examine the overall impact of maintenance policy on the CCF through service and to identify the appropriate maintenance policy from the perspective of CCF control. It shows that the component degradation and maintenance practices could significantly affect the β -factor for CCF probability. The insights are discussed as follows:

- Examination of the nine options for the inspection interval shows that, as expected, with longer inspection intervals, the β -factor monotonically increases. Assuming the same degree of effectiveness, it is straightforward to see that performing inspections more frequently is more likely to prevent potential failure and thus less concurrent failure, leading to smaller β -factor.
- Poor maintenance is associated with low rejuvenation and higher β -factor for CCF probability.
- It is demonstrated that there would be a significant increase in the β -factor with a decrease in the degree of repair quality (i.e., lower rejuvenation). This means that the β -factor would be significantly underestimated when assuming the maintenance practices are perfect, when in practice there is a degree of effectiveness.
- Overall, it is intuitive that frequent high quality maintenance reduces pump degradation, leading to smaller β -factor.

Although perfect maintenance would considerably reduce pump degradation and lead to a small β -factor, the patterns of the β -factor would vary depending on the effectiveness of the maintenance repair. Another sensitivity study was conducted to investigate the effects on β -factor assuming perfect maintenance, but for different inspection intervals, ΔT , in units of hours: {720, 1080, 1440, 1800, 2160, 2520, 2880, 3240, 3600}. The results are summarized in Fig. 15, which shows that mean estimates of the β -factor increase as the inspection intervals

become longer. A comparison of the inspection intervals 720 and 1080 h for perfect and imperfect maintenance regimes from Fig. 15 and Fig. 14(b), respectively, further demonstrates that perfect maintenance would significantly reduce the β -factor. On the other hand, this confirms that the β -factor would be significantly underestimated under the assumption of perfect maintenance, when in practice there is always a degree of maintenance effectiveness. As the β -factor monotonically increases with longer inspection intervals, it is possible to underestimate the β -factor as components degrade even under perfect maintenance practices.

4. Conclusions

This paper presented a novel approach to advance the state-of-the-art CCF research by taking advantage of the recent advances in sensor-based techniques and computation capabilities. The proposed approach models the CCF for components under age-related degradation by superimposing the maintenance impacts on the component degradation evolutions that can be characterized through condition monitoring data. An experimental case study involving three redundant centrifugal pump systems was presented to demonstrate the approach. The pump degradation assessment and condition-based maintenance policy were presented. The significance of CCF events using a component-specific study was discussed, along with the dynamic characteristics of CCF by a sensor-driven scenario and a simulation-based scenario. Sensitivity studies were provided to evaluate the maintenance effects on CCF over lifetime services. The results concluded that the parametric estimates of CCF failure probability may be limited to ideal conditions of perfect maintenance, and age-related degradation could significantly affect the β -factor for CCF probability, leading to underestimation of risks as components degrade. This study also showed the important role of recent advances in sensing techniques and data analytic algorithms in enhancing the current PRA research via online monitoring with reduced uncertainty. Future studies could enhance the degradation modeling involving automatic learning from data representing features or by fusing multiple data sources. Integration of organizational and human error effects would improve the results and provide a more realistic insight into the dynamic properties of CCF. Effect of various degrees of rejuvenation during the renewal process would also be of interest to determine maintenance actions that contribute significantly to premature age-related CCFs. Selection of features that best capture degradations is a subject that can be more formally addressed as opposed to the experiential feature selection used in this study. Finally, probability of multiple failures can be captured through mixture distribution models, where multiple failure mechanisms that degrade the components are competitively progressing toward a final failure.

Acknowledgments

The research presented in this paper was partly funded under the US NRC grant NRCHQ6014G0015. The funding for the experimental effort was provided by the Center for Risk and Reliability at the University of Maryland. The authors appreciate the help from Mr. Jan Muehlbauer on the experimental works and are grateful for comments from the anonymous reviewers, and particularly by constructive suggestions from one of the anonymous reviewers. Any views presented in this paper are those of the authors and do not reflect an official position of the US NRC.

References

- [1] US Nuclear Regulatory Commission. "Guidelines on modeling common-cause failures in probabilistic risk assessment," NUREG/CR-5485, Washington, DC (1998).
- [2] Hokstad P, Rausand M. Common cause failure modeling: status and trends. Handbook of performability engineering. London: Springer; 2008.
- [3] Modarres M, Kaminskiy MP, Krivtsov V. Reliability engineering and risk analysis: a practical guide. CRC press; 2016.

- [4] US Nuclear Regulatory Commission. "Common-Cause failure parameter estimations," NUREG/CR-5497, Washington, DC (1998).
- [5] US Nuclear Regulatory Commission. "Common-cause failure database and analysis system: event data collection, classification, and coding," NUREG/CR-6268, Washington, DC (2007).
- [6] Nuclear Energy Agency. "International common-cause failure data exchange (ICDE): general coding guidelines," NEA/CSNI/R(2011)12, 2012.
- [7] Zitrou A, Bedfor T, Walls L. An influence diagram extension of the unified partial method for common cause failures. *Qual Technol Quant Manag* 2007;4(1):111–28.
- [8] Kelly D, Shen S, Demoss G, Coyne K, Marksberry D. Common-cause failure treatment in event assessment: basis for a proposed new model. Proceedings of the international conference on probabilistic safety assessment and management (PSAM 10). 2010. June 7–11.
- [9] Zheng X, Yamaguchi A, Takata T. α -Decomposition for estimating parameters in common cause failure modeling based on causal inference. *Reliabil Eng Syst Saf* 2013;116:20–7.
- [10] O'Connor A, Mosleh A. A general cause based methodology for analysis of common cause and dependent failures in system risk and reliability assessments. *Reliabil Eng Syst Saf* 2016;145:341–50.
- [11] Fleming KN. On the issue of integrated risk—a practitioner's perspective. Proceedings of the ANS international topical meeting on probabilistic safety analysis. 2005. September 11–15.
- [12] Ebisawa K, Teragaki T, Nomura S, Abe H, Shigemori M, Shimomoto M. Concept and methodology for evaluating core damage frequency considering failure correlation at multi units and sites and its application. *Nucl Eng Des* 2015;288:82–97.
- [13] Modarres M, Zhou T, Massoud M. Advances in multi-unit nuclear power plant probabilistic risk assessment. *Reliabil Eng Syst Saf* 2017;157:87–100.
- [14] Zhou T, Modarres M, Drogue EL. An improved multi-unit nuclear plant seismic probabilistic risk assessment approach. *Reliabil Eng Syst Saf* 2018;171:34–47.
- [15] Stiller JC, Leberecht M, Ganbmantel G, Wielenberg A, Kreuser A, Versteegen C. Common cause failures exceeding ccf groups. Proceedings of the international topical meeting on probabilistic safety assessment and analysis (PSA). 2015. April 26–30.
- [16] Bruck B, Kreuser A, Stiller J, Leberecht M. Extending the scope of ICDE: systematic collection of operating experience with cross component group CCFs. Proceedings of the international conference on probabilistic safety assessment and management (PSAM 13). 2016. October 2–7.
- [17] Vaurio JK. Uncertainties and quantification of common cause failure rates and probabilities for system analyses. *Reliabil Eng Syst Saf* 2005;90(2):186–95.
- [18] Trofaes M, Walter G, Kelly D. A robust bayesian approach to modeling epistemic uncertainty in common-cause failure models. *Reliabil Eng Syst Saf* 2014;125:13–21.
- [19] Kancev D, Cepin M. A new method for explicit modelling of single failure event within different common cause failure groups. *Reliabil Eng Syst Saf* 2012;103:84–93.
- [20] Rejc Z, Cepin M. An extension of multiple greek letter method for common cause failures modeling. *J Loss Prev Process Ind* 2014;29:144–54.
- [21] Holy J, Nitoi M, Dinu I, Burgazzi L. Analysis of common cause failures coupling factors and mechanisms from aging point of view. Proceedings of the APSA Network Task 5 POS Task. 2010. p. 4.
- [22] U.S. NRC. "Evaluations of core melt frequency effects due to component aging and maintenance", NUREG/CR-5510, Washington DC (1990).
- [23] IAEA. "Safety aspects of nuclear power plant ageing", TECDOC-540, Vienna, Austria (1990).
- [24] IAEA. "Ageing management for nuclear power plants, safety guide", No. NS-G-2.12, Vienna, Austria (2009).
- [25] Canadian Nuclear Safety Commission. "Incorporating ageing effects into PSA applications", ENCO FR-(14)-10 (2014).
- [26] US Nuclear Regulatory Commission. "Nuclear plant aging research (NPAR) program plan," Rev.2, NUREG/CR-1144, Washington, DC (1991).
- [27] Meeker WQ, Hong Y. Reliability meets big data: opportunities and challenges. *Qual Eng* 2014;26(1):102–16.
- [28] Zio E. Some challenges and opportunities in reliability engineering. *IEEE Trans Reliabil* 2016;65(4):1769–82.
- [29] Coble JB, Ramuhalli P, Bond LJ, Hines JW, Upadhyaya BR. Prognostics and health management in nuclear power plants: a review of technologies and applications. Richland, WA: Pacific Northwest National Laboratory (PNNL); 2012. No. PNNL-21515.
- [30] American Bureau of Shipping (ABS). "Guidance notes on equipment condition monitoring techniques," Houston, TX (2016).
- [31] IAEA. "Implementation strategies and tools for condition based maintenance at nuclear power plants," TECDOC-1551, Vienna, Austria (2007).
- [32] Wang W, Christer AH. Towards a general condition based maintenance model for a stochastic dynamic system. *J Oper Res Soc* 2000;51(2):145–55.
- [33] Wang P, Youn BD, Hu C. A generic probabilistic framework for structural health prognostics and uncertainty management. *Mech Syst Signal Process* 2012;28:622–37.
- [34] Jardine A, Lin D, Banjevic D. A review on machinery diagnostics and prognostics implementing condition-based maintenance. *Mech Syst Signal Process* 2006;20(7):1483–510.
- [35] Siegel D, Lee J. Reconfigurable informatics platform for rapid prognostic design and implementation: tools and case studies. Proceedings of the Machinery Failure Prevention Technology (MFPT) Conference. 2013. May 13–17.
- [36] D. Verstraete, A. Ferrada, E.L. Drogue, V. Meruane and M. Modarres. "Deep learning enabled fault diagnosis using time-frequency image analysis of rolling element bearings," *Shock and Vibration*, Article ID 5067651 (2017).
- [37] Soylemezoglu A, Jagannathan S, Saygin C. Mahalanobis-Taguchi system as a multi-sensor based decision making prognostics tool for centrifugal pump failures. *IEEE Trans Reliab* 2011;60(4):864–78.
- [38] Vasan ASS, Long B, Pecht M. Diagnostics and prognostics method for analog electronic circuits. *IEEE Trans Ind Electron* 2013;60(11):5277–91.
- [39] Oh H, Azarian MH, Pecht MG. Estimation of fan bearing degradation using acoustic emission analysis and mahalanobis distance. Proceedings of the applied systems health management conference. 2011. May 10–12.
- [40] Si X, Wang W, Hu C, Zhou D. Remaining useful life estimation—a review on the statistical data driven approaches. *Eur J Oper Res* 2011;213(1):1–14.
- [41] Sun J, Zuo H, Wang W, Pecht MG. Prognostics uncertainty reduction by fusing on-line monitoring data based on a state-space-based degradation model. *Mech Syst Signal Process* 2014;45(2):396–407.
- [42] Si X, Wang W, Hu C, Zhou D. Estimating remaining useful life with three-source variability in degradation modeling. *IEEE Trans Reliab* 2014;63(1):167–90.
- [43] Drogue EL, Mosleh A. Bayesian methodology for model uncertainty using model performance data. *Risk Anal* 2008;28(5):1457–76.
- [44] Rabiei E, Drogue EL, Modarres M. A prognostics approach based on the evolution of damage precursors using dynamic Bayesian networks. *Adv Mech Eng* 2016;8(9).
- [45] Arulampalam MS, Maskell S, Gordon N, Clapp T. A tutorial on particle filters for online nonlinear/non-Gaussian Bayesian tracking. *IEEE Trans Signal Process* 2002;50(2):174–88.
- [46] IAEA. "Maintenance, surveillance and in-service inspection in nuclear power plants safety guide," Safety Standards Series No. NS-G-2.6, Vienna, Austria (2002).
- [47] Liu B, Wu S, Xie M, Kuo W. A condition-based maintenance policy for degrading systems with age-and state-dependent operating cost. *Eur J Oper Res* 2017;263(3):879–87.
- [48] US NRC. "Common-Cause failure event insights, volume 3, pumps," NUREG/CR-6819 (2003).
- [49] Beebe RS. Predictive maintenance of pumps using condition monitoring. Elsevier; 2004.
- [50] Wang D, Tse PW. Prognostics of slurry pumps based on a moving-average wear degradation index and a general sequential Monte Carlo method. *Mech Syst Signal Process* 2015;56:213–29.
- [51] Leahy M, Mba D, Cooper P, Montgomery A, Owen D. Experimental investigation into the capabilities of acoustic emission for the detection of shaft-to-seal rubbing in large power generation turbines: a case study. *Proc Inst Mech Eng Part J J Eng Tribol* 2006;220(7):607–15.
- [52] Mba D, Rao RB. Development of acoustic emission technology for condition monitoring and diagnosis of rotating machines; bearings, pumps, gearboxes, engines and rotating structures. *Shock Vib Digest* 2006;38(1):3–16.
- [53] Liu K, Chehade A, Song C. Optimize the signal quality of the composite health index via data fusion for degradation modeling and prognostic analysis. *IEEE Trans Autom Sci Eng* 2017;14(3):1504–14.
- [54] Chehade A, Bonk S, Liu K. Sensory-Based failure threshold estimation for remaining useful life prediction. *IEEE Trans Reliab* 2017;66(3):939–49.
- [55] Wong SM. Common Cause Failure (CCF) analysis and generic CCF data ~ us experience. Proceedings of the IAEA Technical Review Meeting. 2013. November 06–08.